



ACE overexpression in myeloid cells increases oxidative metabolism and cellular ATP

Received for publication, September 30, 2019, and in revised form, December 5, 2019. Published, Papers in Press, December 23, 2019, DOI 10.1074/jbc.RA119.011244

Duo-Yao Cao[‡],  Weston R. Spivia[§], Luciana C. Veiras[‡], Zakir Khan^{¶¶}, Zhenzi Peng[‡], Anthony E. Jones^{||}, Ellen A. Bernstein[‡], Suguru Saito[‡], Derick Okwan-Duodu^{¶¶}, Sarah J. Parker^{§§§},  Jorge F. Giani^{¶¶}, Ajit S. Divakaruni^{||}, Jennifer E. Van Eyk^{§1}, and Kenneth E. Bernstein^{¶¶1,2}

From the [‡]Department of Biomedical Sciences, the [§]Smidt Heart Institute and Advanced Clinical Biosystems Research Institute, the ^{¶¶}Department of Pathology and Laboratory Medicine, and the ^{§§§}Department of Medicine, Cedars-Sinai Medical Center, Los Angeles, California 90048 and the ^{||}Department of Molecular and Medical Pharmacology, UCLA David Geffen School of Medicine, Los Angeles, California 90095

Edited by Qi-Qun Tang

Angiotensin-converting enzyme (ACE) affects blood pressure. In addition, ACE overexpression in myeloid cells increases their immune function. Using MS and chemical analysis, we identified marked changes of intermediate metabolites in ACE-overexpressing macrophages and neutrophils, with increased cellular ATP (1.7–3.0-fold) and Krebs cycle intermediates, including citrate, isocitrate, succinate, and malate (1.4–3.9-fold). Increased ATP is due to ACE C-domain catalytic activity; it is reversed by an ACE inhibitor but not by an angiotensin II AT1 receptor antagonist. In contrast, macrophages from ACE knockout (null) mice averaged only 28% of the ATP levels found in WT mice. ACE overexpression does not change cell or mitochondrial size or number. However, expression levels of the electron transport chain proteins NDUFB8 (complex I), ATP5A, and ATP5 β (complex V) are significantly increased in macrophages and neutrophils, and COX1 and COX2 (complex IV) are increased in macrophages overexpressing ACE. Macrophages overexpressing ACE have increased mitochondrial membrane potential (24% higher), ATP production rates (29% higher), and maximal respiratory rates (37% higher) compared with WT cells. Increased cellular ATP underpins increased myeloid cell superoxide production and phagocytosis associated with increased ACE expression. Myeloid cells overexpressing ACE indicate the existence of a novel pathway in which myeloid cell function can be enhanced, with a key feature being increased cellular ATP.

Angiotensin-converting enzyme (ACE)³ is a zinc-dependent peptidase that is made by endothelium and many other tissues (1). ACE is best known for its effects on blood pressure because it produces the potent vasoconstrictor angiotensin II, and ACE inhibitors are widely used in treating hypertension, heart failure, and other clinical problems (2). Less well-recognized is that ACE cleaves many other peptides beside angiotensin II and plays an important function in several other physiologic processes, including immunity, reproduction, and hematopoiesis (3).

In 1975, it was reported that patients with active sarcoidosis have elevated serum ACE levels (4). We now know that lesional macrophages and macrophage-derived giant cells in virtually all human granulomatous diseases express abundant ACE, including histoplasmosis, leprosy, miliary tuberculosis, granulomatosis with polyangiitis (Wegener's granulomatosis), and others (5–9). Macrophage ACE up-regulation is found in zebra fish granuloma (10). Macrophages in Gaucher's disease make abundant ACE, as do the macrophages found in both early and late stages of human atherosclerotic lesions (11–13). ACE increases when the human monocytic cell line THP-1 is differentiated into macrophages (12). Similarly, when human peripheral blood monocytes are differentiated to macrophages *in vitro*, cell ACE activity increases 9-fold (14). In mice, ACE expression in splenic neutrophils, macrophages, and dendritic cells rapidly increases following *Staphylococcus aureus* or *Listeria monocytogenes* infection (15, 16). Despite these observations, little is known about the functional role of ACE up-regulation in myeloid cells.

Recently, our group investigated two lines of mice in which genetic manipulation was used to selectively increase ACE expression by monocytes and macrophages or by neutrophils (15, 17). In these animals, termed ACE 10/10 and NeuACE

This work was supported by National Institutes of Health Grants P01HL129941 (to K. E. B.), R01AI143599 (to K. E. B.), R21AI114965 (to K. E. B.), R01HL142672 (to J. F. G.), R00HL128787 (to S. J. P.), K99HL141638 (to D. O. D.), T32DK007770 (to L. C. V.), T32CA009056 (to A. E. J.), P30DK063491 (to J. F. G.), R01HL111362 (to J. E. V. E.), and R01HL132075 (to J. E. V. E.) and American Heart Association (AHA) Grants 17GRNT33661206 (to K. E. B.), 16SDG30130015 (to J. F. G.), and 19CDA34760010 (to Z. K.). The authors declare that they have no conflicts of interest with the contents of this article. The content is solely the responsibility of the authors and does not necessarily represent the official views of the National Institutes of Health.

This article contains Tables S1–S3 and Figs. S1–S6.

¹ Supported by the Barbra Streisand Women's Heart Center and holder of the Erika J. Glazer Chair in Women's Heart Health.

² To whom correspondence should be addressed: Depts. of Biomedical Sciences and Pathology, Cedars-Sinai Medical Center, Davis Research Bldg., Rm. 2021, 110 N. George Burns Rd., Los Angeles, CA 90048. Tel.: 310-423-7562; Fax: 310-423-7331; E-mail: Kenneth.Bernstein@cshs.org.

³ The abbreviations used are: ACE, angiotensin-converting enzyme; HBSS, Hanks' balanced salt solution; MRSA, methicillin-resistant *S. aureus*; 2-NBDG, 2-deoxy-2-[(7-nitro-2,1,3-benzoxadiazol-4-yl)amino]-D-glucose; FBS, fetal bovine serum; DAPI, 4',6-diamidino-2-phenylindole; VDAC, voltage-dependent anion channel; MFF, mitochondrial fission factor; TCA, trichloroacetic acid; FCCP, carbonyl cyanide 4-(trifluoromethoxy) phenylhydrazone; TMRE, tetramethylrhodamine, ethyl ester; PMA, 4-phorbol 12-myristate 13-acetate; KO, knockout; FDR, false discovery rate; ATM, atmospheric pressure; CV, column volume; ANOVA, analysis of variance.

ACE increases myeloid cellular ATP expression

mice, the cells overexpressing ACE respond to immune challenge with a consistent enhancement in immune response. For example, ACE 10/10 mice (in which monocytes/macrophages express 16–25-fold WT levels of ACE) resist the growth of B16 melanoma significantly better than WT mice and show increased resistance to infection with *Listeria* or methicillin-resistant *S. aureus* (MRSA) (17, 18). Similarly, NeuACE neutrophils (which express 12–18-fold WT levels of ACE) show increased resistance to MRSA, *Klebsiella pneumoniae*, or *Pseudomonas aeruginosa*, as measured both *in vivo* and in the ability to kill bacteria *in vitro* (15). Both NeuACE neutrophils and ACE 10/10 macrophages make increased levels of NADPH oxidase-dependent superoxide, which contributes to their enhanced killing of bacteria.

To investigate the molecular basis of how ACE overexpression affects cells, we studied the metabolism of such cells. Unexpectedly, in both macrophages and neutrophils, ACE overexpression induces a significant increase in cellular ATP, in levels of Krebs cycle intermediates, and in proteins comprising the electron transport chain. These metabolic changes are due to ACE catalytic activity, as they are reverted to WT levels by treating mice with ACE inhibitors. Our studies find that ACE overexpression by both macrophages and neutrophils is associated with a marked change in the metabolism of cells and that this appears to underpin some of the phenotypic differences between these cells and myeloid cells expressing WT levels of ACE.

Results

Increased ATP in cells overexpressing ACE

Mass spectrometry was used to measure the intermediate metabolites of ACE 10/10 macrophages and NeuACE neutrophils, as well as equivalent cells from WT mice. Thioglycollate-elicited ACE 10/10 macrophages showed 27 significant differences from WT cells (defined as a false discovery rate-adjusted p value <0.01), with 26 metabolites increased in ACE 10/10 (Fig. S1 and Table S1). Only adenosine was diminished. A similar comparison of freshly isolated NeuACE bone marrow neutrophils with equivalent WT cells showed 15 significant differences, with all being increased in the ACE-overexpressing cells. Perhaps most surprising was the increased amounts of adenosine mono-, di-, and triphosphate in both ACE-overexpressing groups (Fig. 1, A and B). In ACE 10/10 macrophages, the increase in cellular ATP, ADP, and AMP was 3.0-, 2.3-, and 2.6-fold the levels in WT cells. In NeuACE neutrophils, there was an equivalent pattern, although the magnitude of the increase (1.9-, 2.1-, and 1.7-fold) was less than in macrophages.

To verify the MS results, we measured levels of cellular ATP chemically in additional samples and found a 2.4- and 1.7-fold increase of ATP in ACE 10/10 macrophages and NeuACE neutrophils ($p < 0.001$; Fig. 1C). Macrophages from ACE heterozygous mice have roughly 2-fold higher levels of ATP as compared with WT ($p < 0.05$), whereas, in stark contrast, cells from ACE knockout (null) mice averaged only 28% of the ATP levels found in WT ($p < 0.01$). For ACE 10/10 macrophages, the ATP/ADP ratio was 2.1 *versus* 1.4 for WT cells, as determined chemically (Fig. 1D).

For NeuACE neutrophils, the ATP/ADP ratio was 3.0 *versus* 1.9 in WT cells.

To examine whether differences in ATP between peritoneal macrophages from ACE 10/10 and WT mice were due to differences in overall cellular protein content, both protein and ATP were measured chemically in another cohort of mice. Whereas ACE 10/10 cells again had significantly more ATP ($p < 0.001$), the protein content of the cells was equivalent to peritoneal macrophages from WT mice (Fig. S2A). As discussed below, we also evaluated the size of ACE 10/10 and WT macrophages and found no differences (Fig. 2E). Finally, whereas the typical preparation of peritoneal macrophages contained 80–90% macrophages by flow cytometry, ATP was also measured in peritoneal macrophages purified to over 90% using an antibody-based negative cell selection protocol. This too showed more ATP in ACE 10/10 macrophages than equivalent WT cells (see Fig. 7A).

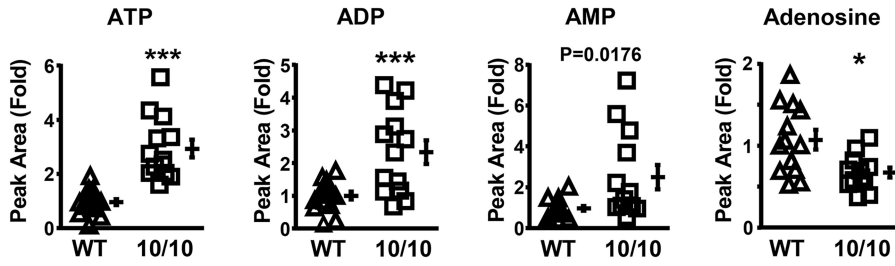
In the above analysis of ATP, neutrophils were obtained from the bone marrow of mice without any additional stimulation. In contrast, peritoneal macrophages were obtained following stimulation with thioglycollate. When resident peritoneal macrophages were isolated without thioglycollate, ACE 10/10 and WT macrophages showed no difference in ATP levels, as did bone marrow-derived macrophages produced *in vitro* (Fig. 2, B and C). Thus, macrophage stimulus affects the level of ATP in ACE 10/10 *versus* WT cells.

The increase of cellular ATP is due to the catalytic activity of ACE. Specifically, when animals were continuously treated for 7 days with the ACE inhibitor ramipril, thioglycollate-induced peritoneal macrophages or bone marrow-derived neutrophils showed ATP levels that were now similar to the cells from WT mice also treated with ramipril (Fig. 1, E and F). In contrast, a similar experiment (7-day treatment) performed with the angiotensin II AT1 receptor antagonist losartan showed no significant effects as compared with equivalent animals not treated with the receptor antagonist. WT mice treated with ramipril had less ATP in macrophages and neutrophils than in WT cells from untreated mice, similar to the result in Fig. 1C with ACE knockout (KO) macrophages.

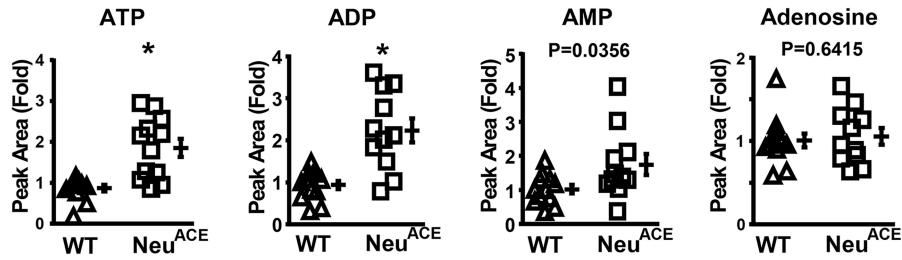
Given the differences in intermediate metabolites observed in cells overexpressing ACE, we examined the quantity of cellular glucose transport proteins GLUT1 and GLUT4 by Western blot analysis. No differences were noted between macrophages and neutrophils overexpressing ACE and equivalent WT cells (Fig. 2A and Fig. S3A). Two means of assessing glucose uptake were used: the uptake of the fluorescent glucose analog 2-deoxy-2-[(7-nitro-2,1,3-benzoxadiazol-4-yl)amino]-D-glucose (2-NBDG), as determined by flow cytometry, and an independent chemical analysis of the uptake of 2-deoxyglucose. Neither assay showed increased glucose uptake in ACE-overexpressing cells as compared with equivalent cells with WT ACE expression (Fig. 2B and Fig. S3B).

Glycolytic flux ultimately produces lactic acid. We assessed lactic acid levels using two approaches. First, MS determination of cellular lactic acid showed no difference in ACE 10/10 macrophages or NeuACE neutrophils as compared with WT cells (Fig. 2C and Fig. 3C). In addition to this static determination of cellular lactic acid, we also measured the production of

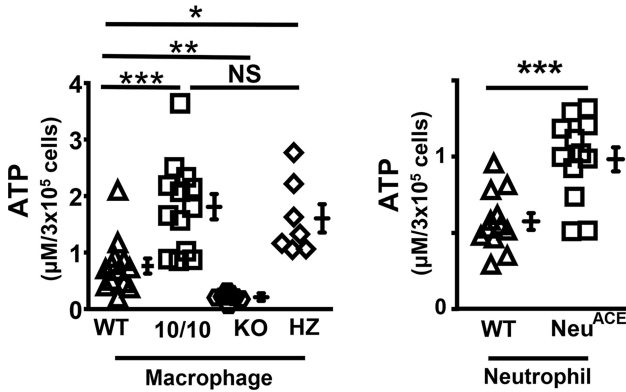
A. Macrophages



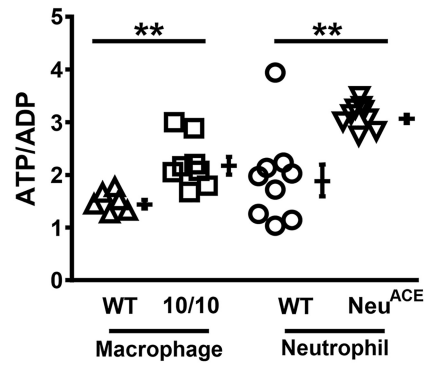
B. Neutrophils



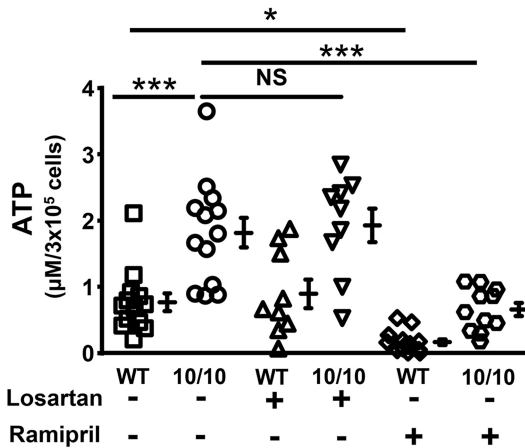
C. ATP concentration



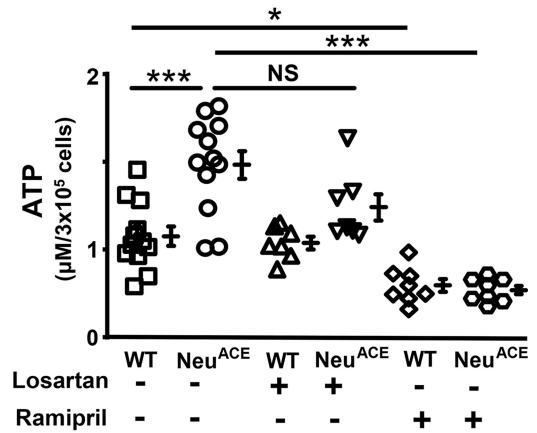
D. ATP/ADP ratio



E. Macrophages



F. Neutrophils



ACE increases myeloid cellular ATP expression

lactic acid by cultured macrophages. Thioglycollate-induced ACE 10/10 and WT macrophages were collected and cultured for 12 h in one of three media: medium with 10% fetal bovine serum (FBS), medium without FBS, and medium without FBS and without glucose. We then assayed the lactate concentration in the culture supernatant via the production of NADH by lactate dehydrogenase (Fig. 2D). This showed a small increase of lactate production by ACE 10/10 cells, but these differences were not significant with the number of samples measured.

A possible explanation for differences in intermediate metabolites could be due to differences in cell size or mitochondrial number. We investigated this using two assays. First, ACE 10/10 macrophages and NeuACE neutrophils were stained with Mitotracker Green and measured by flow cytometry. This assay of mitochondria showed no significant differences between ACE-overexpressing cells and equivalent cells from mice with WT ACE levels (Fig. S4, A and B). In a more extensive analysis, ACE 10/10 macrophages were studied by confocal microscopy following staining of the nuclei, cytoplasm, and mitochondria with 4',6-diamidino-2-phenylindole (DAPI), phalloidin green, and Mitotracker Red, respectively (Fig. 2E). Individual images of cells were then quantified for the number of pixels of cytoplasm and of mitochondria. This analysis showed no differences between ACE 10/10 macrophages and WT cells in cell size, mitochondrial number, mitochondrial size, and mitochondrial number per cell size (Fig. S4C). Further, analysis of ACE 10/10 macrophages by EM showed no significant differences in mitochondrial size or cristae structure (Fig. S4D). This conclusion was supported by using Western blotting to measure total cellular dynamin-like 120-kDa protein (OPA1), voltage-dependent anion channel (VDAC), mitochondrial fission factor (MFF), and TOM20 (Fig. 2F). OPA1, VDAC, and MFF were equivalent between ACE 10/10 macrophages and WT cells. Only TOM20 was different; in ACE 10/10 macrophages, it was 1.4-fold the level of WT cells. Thus, it appears that cell size, the number of mitochondria, and mitochondrial size are not major differentiating features between cells overexpressing ACE and equivalent cells with WT ACE levels.

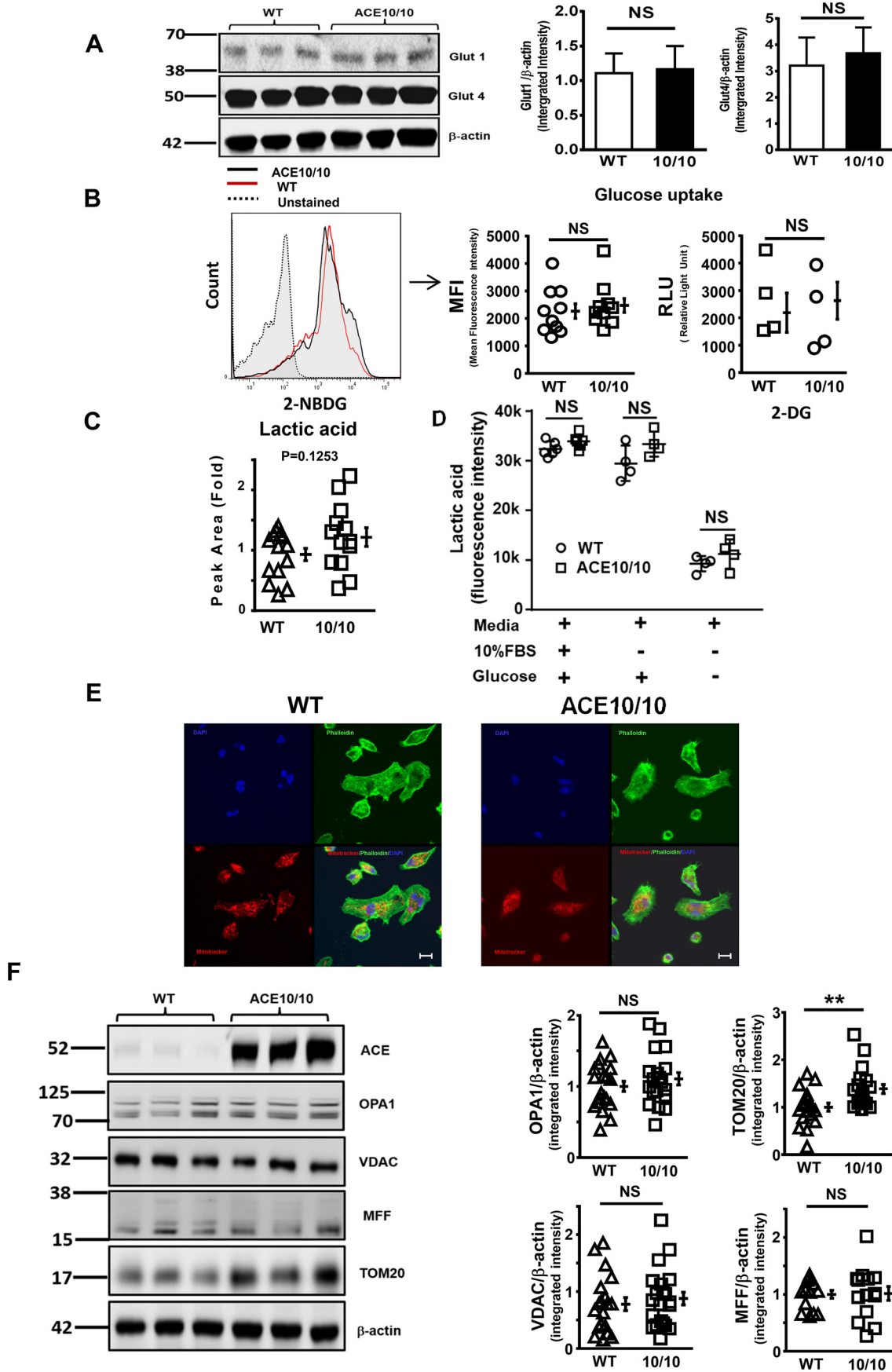
ACE overexpression increases oxidative metabolism

As part of the MS analysis of metabolites, we determined the levels of metabolic intermediates found in the TCA cycle. These data showed that ACE 10/10 macrophages have significantly higher levels of citric acid (3.9-fold), isocitrate (5.2-fold), succinate (1.9-fold), and malate (2.0-fold) (Fig. 3 and Table S1). NAD and FAD in ACE 10/10 macrophages were also 1.6- and

1.5-fold higher than in equivalent WT cells. In neutrophils from NeuACE mice, there was a similar trend, although the differences between cells overexpressing ACE and those with WT ACE levels were less pronounced. Specifically, for citrate, isocitrate, succinate, and L-malate, levels were 2.0-, 1.9-, 1.4-, and 1.5-fold higher in NeuACE neutrophils compared with neutrophils from WT mice. The NeuACE neutrophils also had increased NAD (1.3-fold) and FAD (1.4-fold).

Given the increased concentration of ATP and TCA cycle intermediates in ACE-overexpressing macrophages, we measured cellular respiration to determine whether there were changes in mitochondrial function. Peritoneal macrophages were obtained after thioglycollate injection and then transferred to culture dishes. Following an overnight incubation, cells were gently detached and acutely adhered to an Agilent Seahorse XF96 plate, and respiratory parameters were measured as described previously (Fig. 4, A and B) (19). The rates of ATP production by glycolysis and oxidative metabolism in ACE 10/10 cells were 31 and 27% higher than WT cells. Total ATP production rates by ACE 10/10 cells were 29% higher than WT (11.2 ± 1.00 pmol of ATP/min/1000 cells (ACE 10/10) versus 8.7 ± 1.37 pmol of ATP/min/1000 cells (WT); $p < 0.05$, $n \geq 11$). To investigate whether the change in oxygen consumption upon ACE overexpression was due to direct mitochondrial changes or simply reflected an increased activation state of the cells, we measured maximal oxygen consumption rates with carbonyl cyanide 4-(trifluoromethoxy) phenylhydrazone (FCCP). After blocking ATP synthase with oligomycin, the addition of FCCP measures maximal respiratory rates when mitochondria are disengaged (uncoupled) from ATP synthesis. Indeed, there was a clear difference in maximal oxygen consumption, which averaged 37% higher in ACE 10/10 cells than in WT macrophages (2.81 ± 0.18 pmol of O_2 /min/1000 cells (ACE 10/10) versus 2.05 ± 0.24 pmol of O_2 /min/1000 cells (WT), $p < 0.02$) (Fig. 4C). To further investigate whether the increase in respiration observed upon ACE overexpression was directly due to mitochondrial changes, we permeabilized the plasma membrane of ACE 10/10 and WT macrophages with recombinant perfringolysin O and offered *in situ* mitochondria various respiratory substrates (Fig. 4D) (20, 21). Indeed, ADP-supported respiration was significantly increased in ACE 10/10 in response to pyruvate/malate, glutamate/malate, and succinate/rotenone. Thus, these data indicate a significant increase in respiratory rate in cells overexpressing ACE.

Figure 1. Increased ATP and ADP in macrophages and neutrophils overexpressing ACE. A and B, as measured by MS, cellular levels of ATP, ADP, and AMP increased in ACE 10/10 macrophages (A) and NeuACE neutrophils (B) compared with WT cells. Adenosine decreased in ACE 10/10 macrophages but was equivalent to WT in neutrophils. $n \geq 11$ with the mean \pm S.E. (error bars) indicated. Data were analyzed as described under "Experimental procedures" with the FDR parameter Q set at 1% with significance (discovery) indicated by an FDR-adjusted p value of < 0.01 . *, $p < 0.01$; **, $p < 0.001$; ***, $p < 0.0001$. p values for macrophage and neutrophil AMP and neutrophil adenosine were not significant using these criteria. C, chemical (luminescent) analysis of ATP showed higher levels in ACE 10/10 macrophages, heterozygous (HZ: ACE 10/WT) macrophages, and NeuACE neutrophils compared with WT cells. The increase in ATP is more pronounced in macrophages. In contrast, ATP levels in ACE KO macrophages were lower than WT. The data for WT, ACE 10/10, and NeuACE cells are also used in E and F. $n \geq 7$, mean \pm S.E. with all points representing data from a single animal. Data were analyzed by one-way ANOVA with the Tukey test (macrophages) and unpaired, two-tailed t test (neutrophils): *, $p < 0.05$; **, $p < 0.01$; ***, $p < 0.001$; NS, no significance. D, as measured chemically, the ratio of ATP/ADP was increased in both ACE 10/10 macrophages and NeuACE neutrophils as compared with WT cells. $n \geq 6$, mean \pm S.E. *, $p < 0.05$; **, $p < 0.01$; ***, $p < 0.001$ as determined by unpaired, two-tailed t test. E and F, chemical analysis of ATP in macrophages from ACE 10/10 mice (E) and neutrophils from NeuACE mice (F) treated with the ACE inhibitor ramipril or the angiotensin II AT1 receptor antagonist losartan. The ACE inhibitor, but not the receptor antagonist, reduced ATP levels. Ramipril also significantly reduced ATP levels in WT neutrophils. The data for WT, ACE 10/10, and NeuACE cells are also used in C. All data points represent data from a single mouse. $n \geq 6$, mean \pm S.E. Data were analyzed by one-way ANOVA with the Tukey test. *, $p < 0.05$; **, $p < 0.01$; ***, $p < 0.001$.



ACE increases myeloid cellular ATP expression

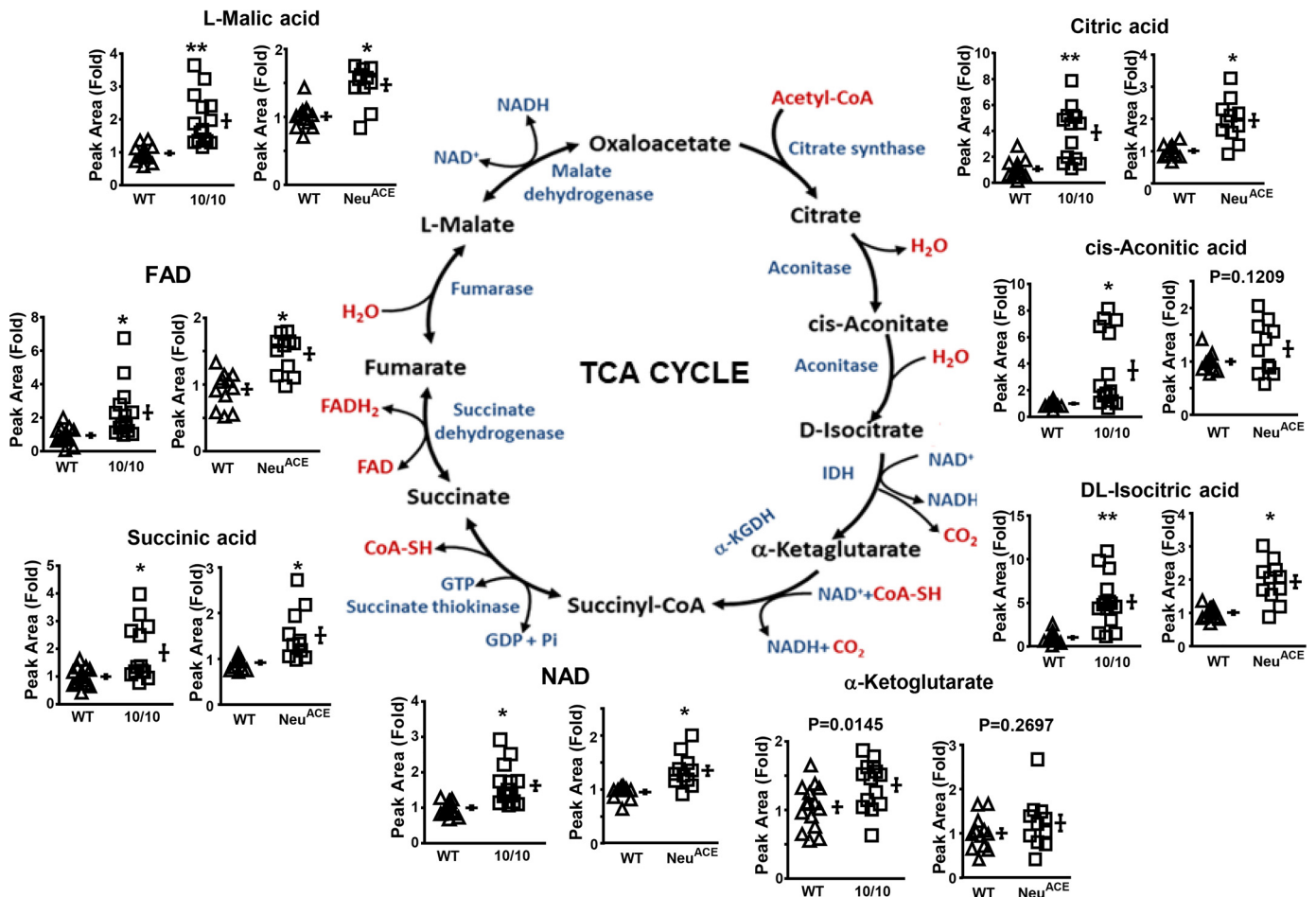


Figure 3. Increased TCA intermediates in macrophages and neutrophils overexpressing ACE. MS was used to measure TCA cycle intermediates in ACE 10/10 macrophages, NeuACE neutrophils, and equivalent cells with WT ACE expression. ACE overexpression is associated with increased levels of several of these intermediates, with differences in citrate, isocitrate, and malate being particularly striking. The magnitude of the increase is more pronounced in macrophages than neutrophils. All data points represent data from a single mouse. $n \geq 10$, mean \pm S.E. (error bars). Data were analyzed using the multiple t test false discovery rate approach described under “Experimental procedures” and in Fig. 1 and Table S1. *, $p < 0.01$; **, $p < 0.001$; ***, $p < 0.0001$. Less significant adjusted p values are given in the figure.

The finding of increased cellular ATP, increased concentrations of TCA intermediates, and increased respiration led us to ask whether ACE affects electron transport chain proteins. These were studied using two different approaches. First, analysis of ACE 10/10 and WT macrophages using MS provided information on 28 proteins associated with mitochondria (Fig. 5A and Table S2). Most striking was the increase in proteins from electron transport complex IV (COX2 and COX4) and complex V (ATP5A) found in ACE 10/10. TOM20 was also significantly increased in ACE 10/10 macrophages.

As a second means of assessing electron transport chain protein, we used Western blot analysis with six antibodies directed against a protein present in each of the five electron transport

chain complexes (NDUFB8, SDHB, UQCRC2, COX1, ATP5A, and ATP5 β) of ACE 10/10 macrophages and NeuACE neutrophils (Fig. 5, B and C). An equivalent study used WT cells. In both macrophages and neutrophils overexpressing ACE, there was a significant increase in the proteins from electron transport complex I (NDUFB8) and complex V (ATP5A and ATP5 β) as compared with WT data. This is despite the fact that neutrophils predominantly use glycolysis rather than oxidative phosphorylation to generate ATP (22). ACE 10/10 macrophages also had an increase of COX1 from electron transport complex IV. Thus, these data showing an increase of a subset of electron chain proteins are complementary to the increased respiratory rate found in ACE 10/10 macrophages.

Figure 2. Glucose transport and glycolytic metabolites in NeuACE and WT neutrophils. A, Western blot analysis of the glucose transporters Glut1 and Glut4 in WT and ACE 10/10 macrophages (left). There is no significant difference (NS) between the two groups (right). $n \geq 6$, mean \pm S.E. (error bars). Analysis was by unpaired, two-tailed t test. B, uptake of the glucose analogue 2-NBDG in ACE 10/10 and WT cells measured by flow cytometry (left and center). Uptake of the glucose analogue 2-deoxyglucose measured by luminescence (right). $n \geq 4$, mean \pm S.E. Analysis was by unpaired, two-tailed t test. C, determination of WT and ACE 10/10 macrophage lactic acid by MS. All data points represent data from a single mouse. $n \geq 13$, mean \pm S.E. The FDR-adjusted p value is from Table S1. D, measurement of lactic acid production by ACE 10/10 and WT neutrophils in medium with and without FBS and glucose. $n \geq 4$, mean \pm S.E., where each point represents a separate animal. Analysis was by two-way ANOVA with the Sidak test. E, staining of WT and ACE 10/10 macrophages to identify nuclei (DAPI; blue), cytoplasm/cytoskeleton (phalloidin; green), and mitochondria (Mitotracker Red). Scale bar, 10 μ m. F, Western blotting was used to identify cellular ACE, OPA1, VDAC, MFF, TOM20, and β -actin in WT and ACE 10/10 macrophages. Only TOM20 was different (1.4-fold higher; **, $p < 0.01$) between ACE-overexpressing cells and WT. In the graphs (right), each point represents data from a single mouse. $n \geq 10$, mean \pm S.E. Analysis was by unpaired, two-tailed t test.

Elevated cellular ATP is associated with an increased immune response

ACE is a single polypeptide chain, but it is composed of two homologous catalytic domains termed the N- and C-domains (1). We previously described three transgenic mouse lines in which myeloid cells overexpress ACE with both domains active or ACE with point mutations catalytically inactivating either the N- or C-domains (24). These mice are called Tg-ACE, Tg-NKO, and Tg-CKO. The Tg-ACE and Tg-NKO mice strongly resist melanoma tumor growth, similar to the increased immune response present in ACE 10/10 mice. Macrophages from these mice overexpress superoxide when exposed to melanoma cells (24). In contrast, the Tg-CKO mice and Tg-CKO macrophages are essentially no different from control WT mice and WT macrophages in tumor resistance and superoxide production.

To study the relationship between ATP levels and immune resistance, we measured cellular ATP in macrophages from ACE 10/10, WT, Tg-ACE (abbreviated JWT), Tg-NKO (JNKO), and Tg-CKO mice (JCKO) (Fig. 6A). Similar to the immune phenotype, ACE 10/10, Tg-ACE, and Tg-NKO mice have increased cellular ATP, as compared with Tg-CKO or WT animals. Further, the production of superoxide in response to 4-phorbol 12-myristate 13-acetate (PMA), a key feature distinguishing ACE 10/10 cells from WT, also showed a similar grouping where increased production was observed in ACE 10/10, Tg-ACE, and Tg-NKO macrophages, whereas production in Tg-CKO macrophages was similar to WT cells (Fig. 6B). Further, analysis of mitochondrial proteins by Western blotting showed a similar pattern: macrophages from ACE 10/10, Tg-ACE, and Tg-NKO express more ATP5A, ATP5 β , and NDUFB8 protein than WT or Tg-CKO (Fig. 6C).

To further investigate the role of ATP in the phenotype of cells overexpressing ACE, we treated ACE 10/10 and WT macrophages, as well as NeuACE and WT neutrophils, with oligomycin. This inhibitor of ATP synthase reduced cellular ATP concentrations such that the macrophages overexpressing ACE had ATP levels very similar to WT cells (Fig. 7A). The treated NeuACE neutrophils had ATP levels similar to treated WT cells but less than untreated WT (Fig. 7C). When ACE 10/10 macrophages were challenged with PMA and superoxide production was measured, treatment with oligomycin eliminated the difference between these cells and WT cells (Fig. 7B). When NeuACE neutrophils were studied, the 5- and 10-min time points showed results similar to that of WT (Fig. 7D). However, WT superoxide production deteriorated by 15 min, making analysis uncertain. Nonetheless, these data, and particularly the results with macrophages, suggest a direct link between high cellular ATP and one of the phenotypic characteristics of the ACE-overexpressing cells.

To further examine this, we measured phagocytosis of *E. coli* by thioglycollate-induced peritoneal macrophages from ACE 10/10, WT, and ACE KO mice. After harvest, cells were cultured for 2 h with fluorescein-labeled fragments of *Escherichia coli* either with or without oligomycin (10 μ g/ml). After washing, cells were stained for CD11b and F4/80 and analyzed by flow for the mean fluorescence of the fluorescein signal, which

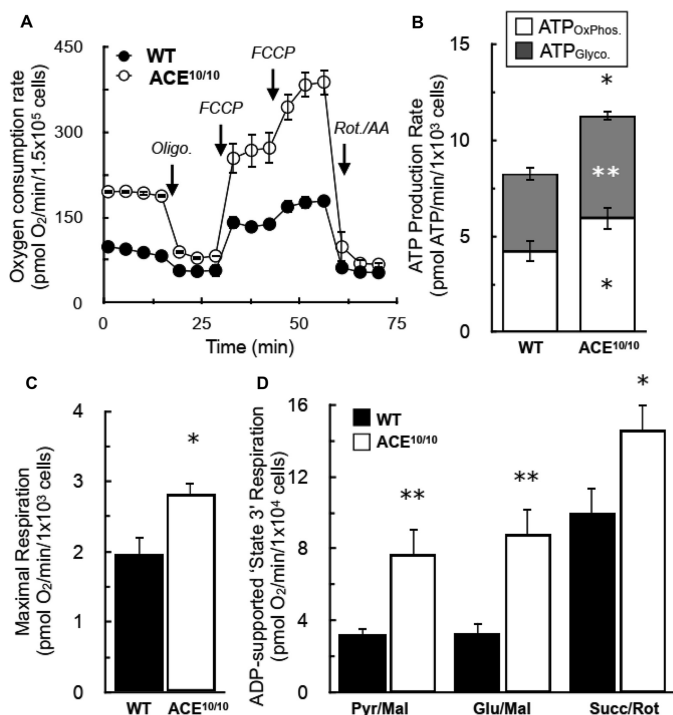
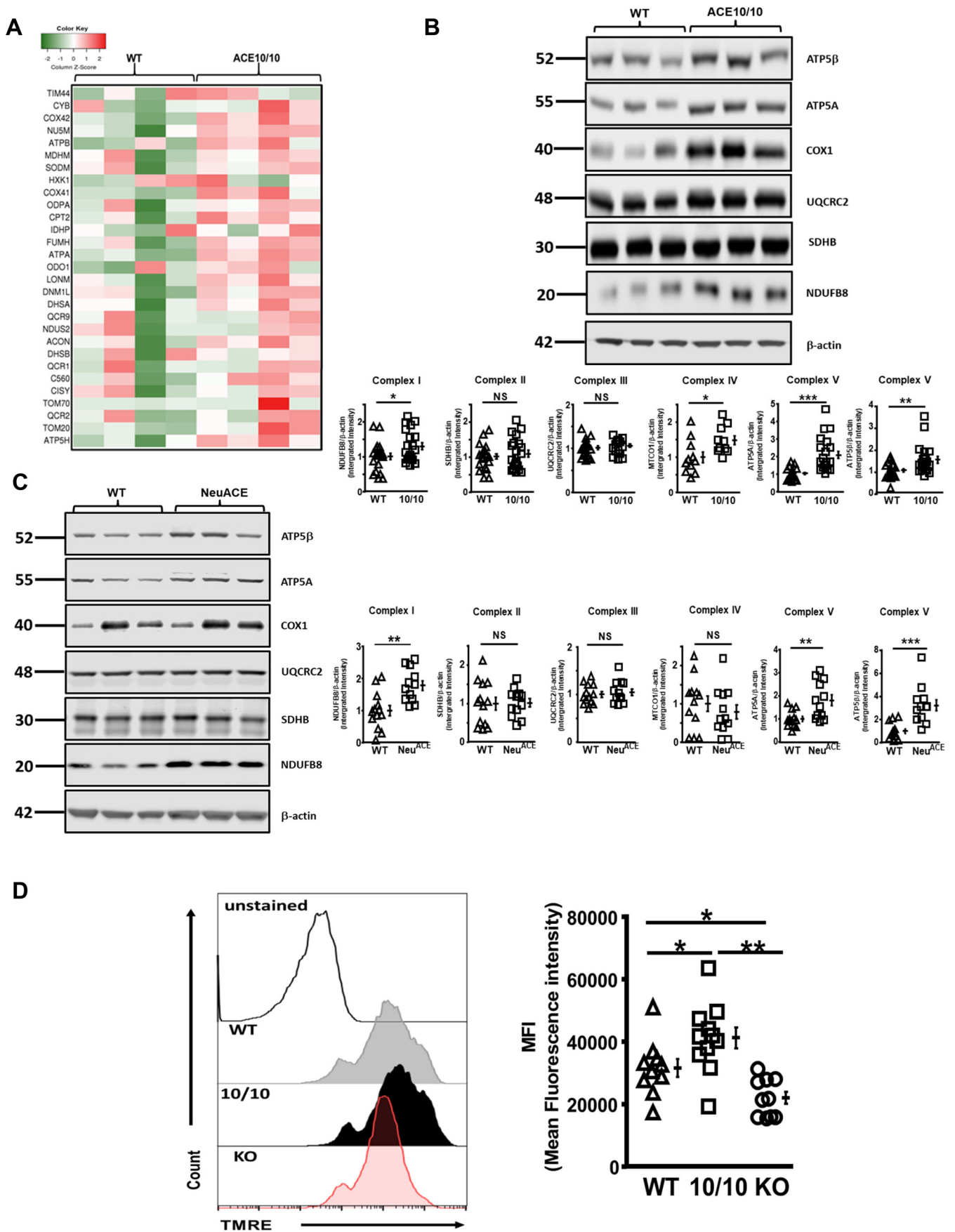


Figure 4. Increased respiration in ACE 10/10 macrophages. A, respiration was measured in WT and ACE 10/10 macrophages with an Agilent Seahorse XF analyzer. Shown is a representative trace of oxygen consumption in peritoneal macrophages under basal conditions and in response to mitochondrial effectors oligomycin, FCCP, and rotenone/antimycin A. B, rates of ATP production from glycolysis and oxidative phosphorylation. C, the maximal respiratory capacity from Seahorse XF analysis. Metabolic measurements were increased in ACE 10/10 cells compared with WT. D, respiration of ACE 10/10 and WT macrophages associated with ADP conversion into ATP in the presence of either pyruvate/malate, glutamate/malate, or succinate/rotenone. Respiration was increased in ACE 10/10 macrophage under all conditions. Data in A–D are presented as the mean \pm S.E. (error bars), where $n \geq 9$ mice/group; *, $p < 0.05$; **, $p < 0.01$ after analysis using unpaired, two-tailed t test.

Mitochondrial production of ATP is driven by the difference in membrane potential across the inner mitochondrial membrane. This was assessed by flow analysis of macrophages from ACE 10/10, WT, and ACE knockout mice after staining with the mitochondrial dye tetramethylrhodamine, ethyl ester (TMRE) (23). In this assay, increased membrane potential results in increased fluorescence. We saw that, as compared with WT cells, macrophages from ACE 10/10 mice had a 24% increase of mean fluorescence intensity (increased $\Delta f/m$), whereas macrophages from ACE knockout mice had a 30% decrease of mean fluorescence intensity (Fig. 5D, $p < 0.05$).

Whereas the NeuACE mice are transgenic, the ACE 10/10 mice were made by substituting the promoter of the endogenous ACE gene. T and B cells from ACE 10/10 do not make increased ACE, but to study whether the genetic manipulation had a generalized effect on all hematopoietic cells, we measured ATP levels and selective electron transport proteins in these cells (Fig. S5, A and B). This showed that ACE 10/10 T and B cells have levels of cellular ATP and mitochondrial proteins equivalent to those of WT cells. Western blotting was also used to assess the level of electron transport proteins in the spleen, heart, lung, liver, kidney, and skeletal muscle of ACE 10 (Fig. 5C). As with lymphocytes, there was no difference between ACE 10/10 and WT mice.

ACE increases myeloid cellular ATP expression



is indicative of phagocytosis (Fig. 7E). Without oligomycin, ACE 10/10, WT, and ACE KO cells showed increased, normal, and reduced levels of phagocytosis. Oligomycin reduced the level of phagocytosis of ACE 10/10 cells to WT levels (Fig. 7F). These experiments again indicate a direct link between high cellular ATP and the enhanced immune response of ACE-overexpressing cells.

Discussion

ACE was discovered in the mid-1950s during studies on the biochemistry of blood pressure control (1, 25). In 1975, the discovery that active sarcoidosis is associated with elevated serum ACE levels was useful clinically but never led to fundamental insight into why myeloid cells within granuloma increased production of this protein (4). Beyond granuloma, macrophages participating in the chronic inflammation accompanying human atherosclerotic lesions also make significant ACE (12). Further, recent analysis shows that WT macrophages (and neutrophils) acutely exposed to a bacterial infection such as MRSA rapidly and significantly increase ACE expression (Fig. S6) (15). But it was the finding that mice overexpressing ACE in macrophages or independently in neutrophils are far more resistant to a variety of disease processes, including tumors (adaptive immunity), bacterial infections (innate immunity), and even the chronic neurotoxicity and neuroinflammation associated with Alzheimer's-like disease, that showed that myeloid cell ACE has a very substantial effect on myeloid cell immune function (3, 15, 18, 24, 26). How ACE increases myeloid cell function is not understood, but we posit that the effects seen in the overexpression models are exaggerations of the natural effects of myeloid ACE expression. The reduced phagocytic ability of macrophages or neutrophils without ACE expression is consistent with this model (Fig. 7G) (15).

Here, we describe a host of metabolic changes in both macrophages and neutrophils overexpressing ACE derived from study of two separate lines of mice. What is striking is that virtually all changes in metabolic intermediates increase in these cells. A prominent change is the significant increase in cellular ATP. This finding, verified by MS and chemical analysis in two separate lines of mice, depends on ACE catalytic activity: cells with high, normal, or no ACE have high, normal, or low ATP. Further, treatment of mice with an ACE inhibitor reduces cellular ATP. In contrast, an angiotensin II AT1 receptor antagonist does not affect myeloid cell ATP. Recent analysis has confirmed that ACE is a promiscuous peptidase with hundreds of substrates (27), but the effect of ACE on myeloid cells is not due to angiotensin peptides, given the repeated ineffectiveness of AT1 receptor antagonists, renin inhibition, and genetic abla-

tion of all angiotensin peptides on the immune phenotype of ACE-overexpressing myeloid cells (3, 15, 17). Further, the phenotype of ACE-overexpressing myeloid cells appears independent of bradykinin or substance P (15, 24, 28).

As concerns cellular ATP, NeuACE neutrophils exhibit an increase without activation, whereas for peritoneal ACE 10/10 macrophages, some degree of stimulation such as thioglycollate appears required, as indicated by the finding that resident peritoneal macrophages have ATP levels equivalent to WT cells. The basis for this difference is not yet understood. Bone marrow-derived ACE 10/10 macrophages overexpress ACE but do not overexpress ATP. Such cells are produced under nonphysiologic conditions *in vitro*. Perhaps the ACE substrate that affects metabolism is not available under the conditions used to generate these cells.

Given that ACE can affect myeloid cell ATP, we examined metabolic pathways that may be responsible. This revealed an up-regulation of metabolic intermediates comprising the citric acid cycle, particularly citrate, isocitrate, succinate, and malate. Increases in these metabolites are present in both macrophages and neutrophils, although the effect is less in neutrophils, as these cells derive most ATP from glycolysis (22). Published reports have detailed the metabolic changes observed in several different stimulated immune cells (29–33). Such studies describe a change in cell metabolism characterized by increasing glycolysis to support ATP production rates and a repurposing of the citric acid cycle to produce signaling metabolites, such as succinate and itaconate (30). It appears that the metabolic phenotype we observe in myeloid cells overexpressing ACE is different in that we did not observe a large burst of glycolysis. In ACE 10/10 macrophages, there is a small percentage increase in glycolytic activity indicated by Seahorse analysis. But glucose uptake and lactate were not increased compared with WT cells in other assays. For NeuACE neutrophils, both glucose uptake and lactate measured by MS were equivalent to WT cells. What our data do establish is that there are changes in the cellular protein content of some electron transport chain components. In particular, there is a consistent increase in components of electron transport complex V (ATP synthase) in both macrophages and neutrophils. Macrophages also show an increase in complex IV. Further, measurement of mitochondria membrane potential showed an increase in ACE 10/10 macrophages and a decrease in ACE KO macrophages as compared with WT cells. Thus, it appears that ACE activity directly correlates with mitochondrial membrane potential. These data are consistent with the Seahorse observations that

Figure 5. Mitochondrial protein in ACE 10/10 and WT macrophages. A, heat map showing the expression of 29 mitochondrial proteins determined by MS. Mean Z scores were created for each protein using GraphPad Prism version 7.04. Darker shades of red represent increased amounts of protein. Data are from the analysis of cells from 4 mice/group. The mean data for all proteins are listed in Table S2. B and C, Western blot analysis was used to measure selected proteins from the five mitochondrial electron transport complexes. As compared with cells with WT levels of ACE, ACE 10/10 macrophages (B) and NeuACE neutrophils (C) make increased levels of the electron transport complex V proteins ATP5A and ATP5 β and the complex I protein NDUFB8. ACE 10/10 macrophages also make more of the complex IV protein COX1. Individual points represent data from a single mouse. $n \geq 10$, mean \pm S.E. (error bars). Analysis was by unpaired, two-tailed t test: *, $p < 0.05$; **, $p < 0.01$; ***, $p < 0.001$; NS, no significance. D, mitochondrial membrane potential. Cultured peritoneal macrophages from WT, ACE 10/10, and ACE KO mice were incubated with TMRE (100 nM) for 20 min and then analyzed by flow. Histograms are representative examples of mean fluorescence intensity (MFI) for WT, ACE10/10, and ACE KO cells. In the graph, each point represents data from a single mouse. Compared with the average for WT cells, macrophages from ACE 10/10 had a 24% increase of $\Delta\psi_m$, whereas macrophages from ACE KO had a 30% decrease in $\Delta\psi_m$. $n \geq 9$ mice, mean \pm S.E. Analysis was by one-way ANOVA with the Tukey test: *, $p < 0.05$; **, $p < 0.01$.

ACE increases myeloid cellular ATP expression

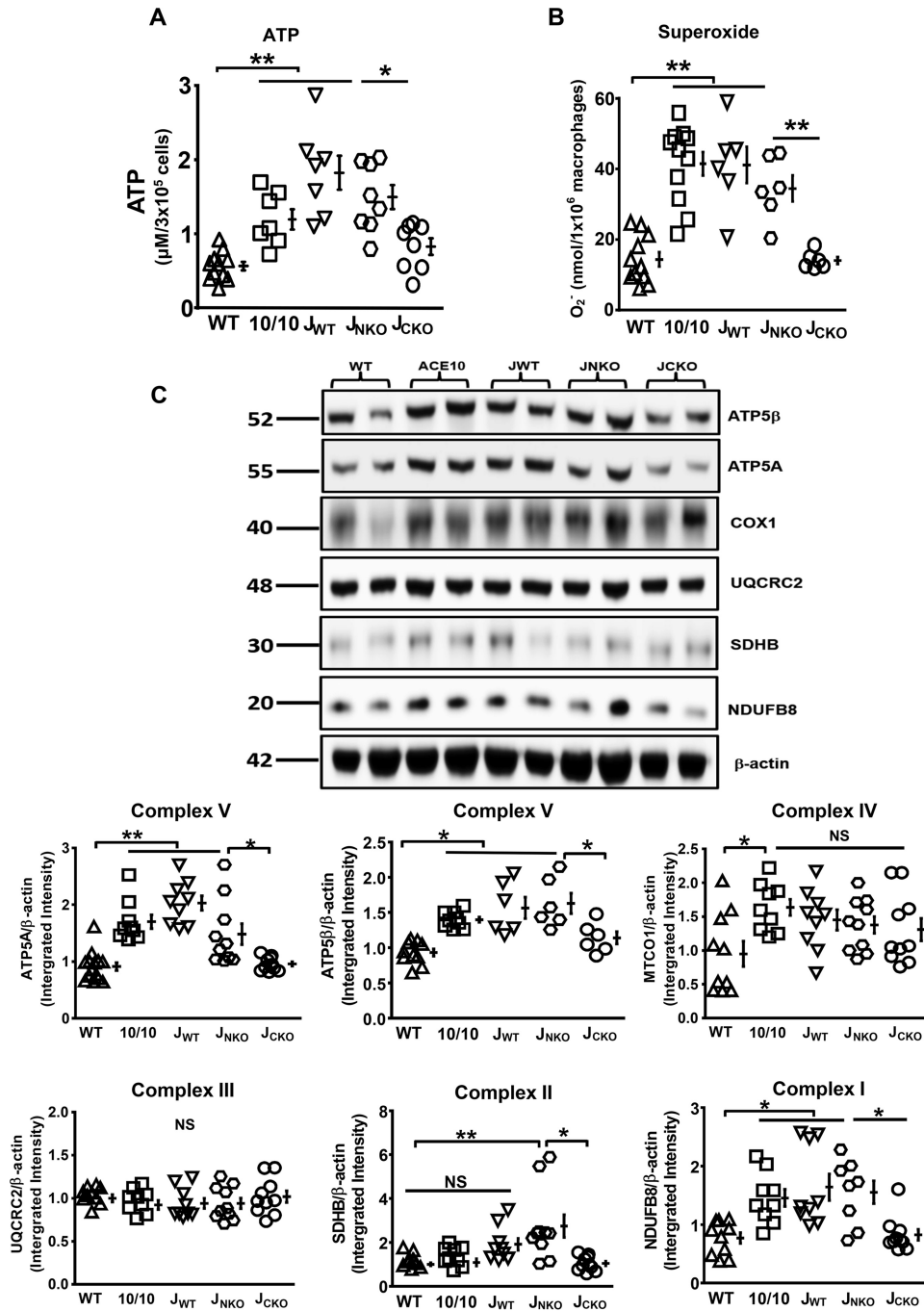


Figure 6. Increased cellular ATP and superoxide production in cells overexpressing the ACE C-domain. The transgenic mouse lines JWT, JNKO, and JCKO overexpress ACE in myeloid cells. In JWT, both ACE catalytic domains are active, whereas in JNKO and JCKO mice, the transgenic ACE lacks activity in the N- and C-domains, respectively. A and B, cellular ATP (A) and superoxide production (B) in macrophages of WT mice, ACE 10/10, JWT, JNKO, and JCKO. Overexpression of ACE with a catalytically active C-domain in ACE 10/10, JWT, and JNKO mice is associated with increased ATP and superoxide. JCKO cells are similar to WT. Each point represents one mouse. $n \geq 6$, mean \pm S.E. (error bars). *, $p < 0.05$; **, $p < 0.01$, determined by one-way ANOVA with the Tukey test. C, Western blot analysis was used to evaluate selected proteins from the five mitochondrial electron transport complexes. As compared with cells with WT levels of ACE, overexpression of ACE with a catalytically active C-domain (ACE 10/10, JWT, and JNKO) is associated with increased ATP5A, ATP5 β , and NDUFB8. $n \geq 6$ mice, mean \pm S.E. *, $p < 0.05$; **, $p < 0.01$; NS, no significance, determined by one-way ANOVA with the Tukey test.

the maximal rate of oxidative respiration is significantly increased in ACE-overexpressing macrophages.

An important question is whether the increased cellular ATP in myeloid cells overexpressing ACE is important in the enhanced immunologic phenotype of these cells. Although this is difficult to prove with certainty, there are two lines of evidence suggesting that ATP is critical for at least some aspects of

the immune response. One is the association between the phenotype of the Tg-NKO and Tg-CKO mouse models and their immune behavior. In both transgenic lines, ACE is equivalently overexpressed by myeloid cells (24). Further, both lines make full-length ACE protein, with the only difference being the presence of point mutations eliminating either ACE N-domain or C-domain zinc binding and catalytic ability. Previously, we

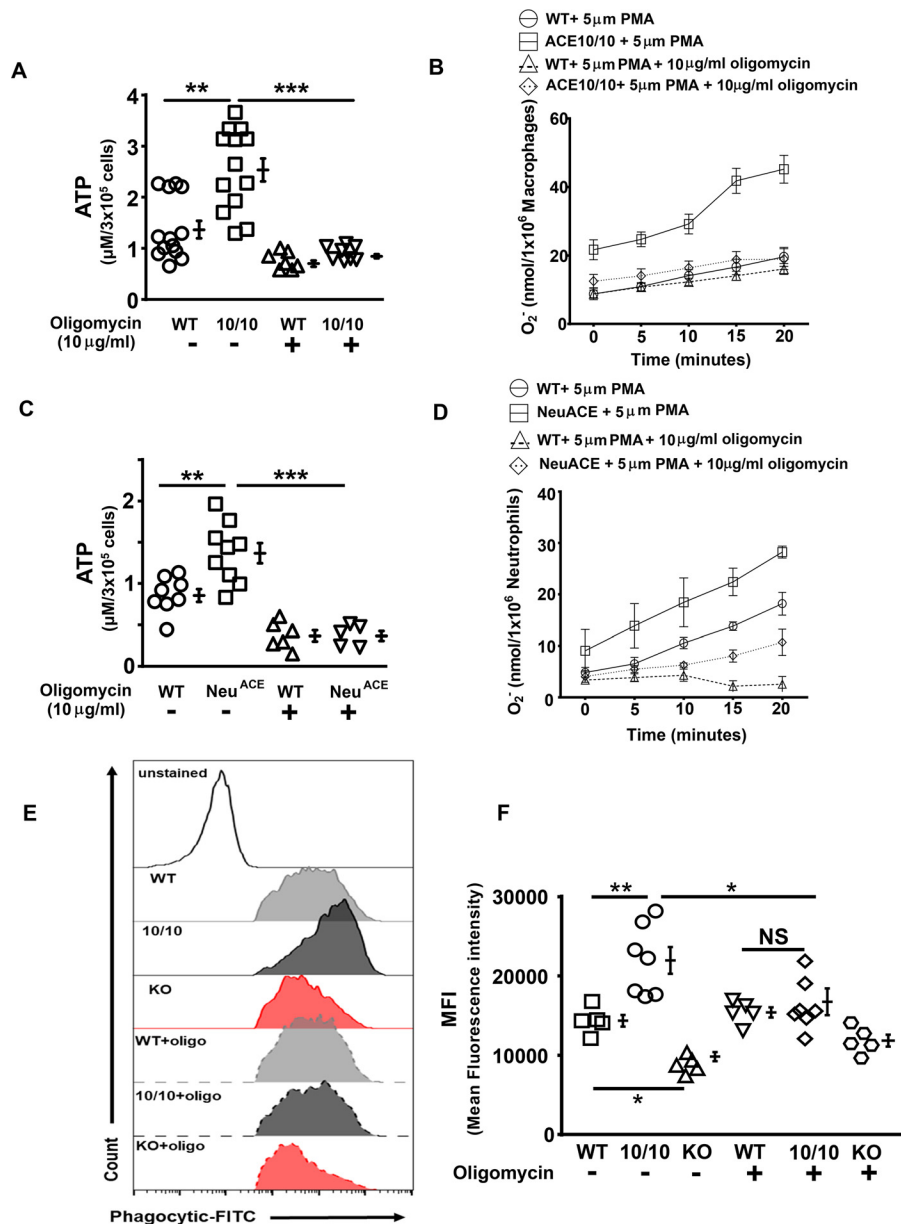


Figure 7. Decreasing ATP in ACE-overexpressing cells reduces superoxide production and phagocytosis to WT levels. A and B, ACE 10/10 macrophages and WT cells were treated with the ATP synthase inhibitor oligomycin (10 μ g/ml) for 20 min. Cellular ATP levels (A) and PMA-induced production of superoxide (B) were measured. C and D, a similar experiment was performed using NeuACE neutrophils and WT cells. For A–D, $n \geq 5$ mice, mean \pm S.E. (error bars). A and C were studied by one-way ANOVA with the Tukey test. **, $p < 0.01$; ***, $p < 0.001$. E and F, peritoneal macrophages from WT, ACE 10/10, and ACE KO mice were cultured with fluorescein-labeled *E. coli* particles with or without oligomycin (10 μ g/ml) for 2 h. Analysis of green fluorescence in CD11b⁺F4/80⁺ cells is shown in E, whereas the mean fluorescence intensity (MFI) is plotted in F. $n \geq 5$ mice, mean \pm S.E. Analysis was by one-way ANOVA with the Tukey test: *, $p < 0.05$; **, $p < 0.01$; NS, no significance.

found that the anti-tumor resistance of Tg-CKO mice is similar to that of control WT mice, animals without ACE overexpression (24). In contrast, the Tg-NKO mice have increased tumor resistance, essentially equivalent to transgenic mice overexpressing an ACE protein with both catalytic domains being active. We now find that macrophages from Tg-NKO mice have an elevated cellular concentration of ATP, as well as increased macrophage production of superoxide. In contrast, macrophages from Tg-CKO mice have both ATP levels and superoxide production similar to that of control WT cells. Thus, increased cellular ATP levels, increased ability to produce superoxide, and a better immune response against tumors

all map to cells with an active ACE C-domain. In contrast, cells with an active ACE N-domain have normal levels of ATP, superoxide production, and immune phenotype.

Another line of evidence associating increased ATP with the enhanced immune phenotype is the experiments in which we used oligomycin to equilibrate the ATP content of ACE 10/10 macrophages and NeuACE neutrophils to WT cells. This manipulation also reduced production of superoxide to the levels of equivalently treated WT cells. Finally, oligomycin treatment reduced the normally increased phagocytic ability of ACE 10/10 macrophages to that of drug-treated WT cells. Thus, it appears that increased cellular ATP is advantageous and under-

ACE increases myeloid cellular ATP expression

pins some of the enhanced immune performance of myeloid cells overexpressing ACE.

Historically, the production of angiotensin II by ACE and the effects of angiotensin II on blood pressure were so important that they eclipsed the role of ACE in other physiologic processes. Whereas ACE 10/10 and NeuACE mice overexpress ACE in myeloid cells to a degree beyond that observed under physiologic conditions, there is now abundant evidence in both humans and WT mice that myeloid cells do increase ACE production when immunologically challenged (3). We posit that the increased ACE helps the adaptation of myeloid cells to inflammatory conditions, and our data now show that an important part of how ACE operates is through changes in cell metabolism. We view the overexpression of ACE in ACE 10/10 and NeuACE myeloid cells as equivalent to the typical use of superphysiologic concentrations of steroids in clinical medicine. The surprising phenotype of mice overexpressing ACE indicates the existence of an unknown pathway in which myeloid cell function can be enhanced, with a key feature being increased cellular ATP. To advance potential clinical utility, knowing what peptide substrate of ACE enhances myeloid function will be useful, but equally useful—and perhaps easier to uncover—will be an understanding of the intracellular changes that promote increased cellular ATP.

Experimental procedures

Mice

All mouse strains were described previously and were on a C57BL/6 background through either breeding to C57BL/6 mice for more than 10 generations (ACE 10/10) or through direct creation in C57BL/6 (NeuACE) (15, 17, 24). Mice were 10–15 weeks old. Neutrophils were isolated from bone marrow following sacrifice. Macrophages were collected 4 days following a 3-ml peritoneal injection of 3% thioglycollate, which is important to observe the phenotype (17). Macrophages were collected, washed, and purified by either Percoll gradient (72 and 36%; GE Healthcare) or a mouse Macrophage Isolation Kit Peritoneum (Miltenyi Biotec) following the manufacturer's instructions. In some experiments, macrophages were isolated following lavage of the peritoneum with medium B (HBSS containing penicillin (100 units), streptomycin (100 μ g/ml), 10 mM HEPES, pH 7.4, BSA (0.06%), and NaHCO_3 (0.0375%)). Mice received the ACE inhibitor ramipril (36.3 mg/liter) (Sigma) or the AT-1 receptor antagonist losartan (600 mg/liter) (LKT LABS) in drinking water for 1 week. All animal experimental protocols were approved by the Cedars-Sinai Institutional Animal Care and Usage Committee.

Analysis of intracellular ATP content and ATP/ADP ratios

To measure intracellular ATP or the ATP/ADP ratio, macrophages or neutrophils were collected from the peritoneal cavity after thioglycollate or from bone marrow, washed twice in cold PBS, pelleted, and then resuspended in RPMI 1640. For ATP, 3×10^5 cells were put in wells of a 96-well plate, and ATP was measured using the CellTiter-Glo 2.0 kit (Promega) as recommended by the manufacturer. ATP/ADP ratios in macrophages and neutrophils were determined using the EnzyLight™ ADP/ATP ratio assay kit (BioAssay Systems) with the protocol rec-

ommended by the manufacturer. In the assays in which protein was measured, a separate aliquot of 1×10^5 cells was lysed with radioimmune precipitation assay buffer, and protein was measured using a Pierce BCA kit (Thermo Fisher Scientific).

Metabolomics

After collection and washing, cell pellets containing 10 million purified macrophages or neutrophils were treated with 500 μ l of cold 40% acetonitrile, 40% methanol, 20% water. Then samples were vortexed vigorously for 15 min at 4 °C and spun at $10,000 \times g$ for 10 min at 4 °C, and the supernatant was removed and placed in a SpeedVac until dry. To resuspend, 20 μ l of methanol was added, followed by vortexing, and finally, 80 μ l of water was added along with a final vigorous vortex. For LC-MS analysis, 4 μ l of sample volume were injected.

Cell metabolite extractions were analyzed with an Agilent 6470A triple quadrupole mass spectrometer, operating in negative mode, connected to an Agilent 1290 ultra-high-performance liquid chromatography (UHPLC) system (Agilent Technologies, Santa Clara, CA). Mobile phases are of HPLC or LC-MS grade reagents. Buffer A is water with 3% methanol, 10 mM tributylamine, and 15 mM glacial acetic acid. Buffers B and D were isopropyl alcohol and acetonitrile, respectively. Finally, Buffer C was methanol with 10 nM tributylamine and 15 mM glacial acetic acid. The analytical column used was an Agilent ZORBAX RRHD Extend-C18 1.8 μ m 2.1 \times 150 mm coupled with a ZORBAX Extend Fast Guard column for ultra-high-performance liquid chromatography Extend-C18, 2.1 mm, 1.8 μ m. The MassHunter Metabolomics dMRM database and method was used to scan for polar metabolites within each sample (Agilent Technologies).

The resulting chromatograms were visualized in Agilent MassHunter Quantitative Analysis for QQQ (Agilent Technologies). The final peak areas were manually checked for consistent and proper integration. Data files have been deposited at MassIVE (massive.ucsd.edu;⁴ accession number MSV0000-84640). They can be downloaded from ftp://massive.ucsd.edu/MSV000084640/ and can be opened with Agilent MassHunter or converted to an open file type.

-Fold changes for the metabolites of WT and ACE-overexpressing samples were determined for each experiment. First, for each sample, the WT peak areas for each metabolite were determined using Agilent Mass Profiler Professional (Agilent Technologies). A WT average area for each metabolite and for each experiment was then calculated, and each WT sample metabolite was compared with the WT average as follows: each WT sample metabolite -fold change = WT (metabolite sample area)/WT (metabolite average area for the experiment). For the ACE-overexpressing samples, the -fold change for each metabolite and for each experiment was determined as follows: each ACE sample metabolite -fold change = ACE (metabolite sample area)/WT (metabolite average area for the experiment). For final analysis, -fold change data from all mice from five experiments for macrophages and four experiments for neutrophils were assembled, and mean -fold change for each metabolite was determined (Fig. S1). To assess significance of differences (discovery), data were analyzed using GraphPad Prism 8.0 and multiple *t* test where no consistent S.D. was assumed. We used false

discovery rate (FDR) analysis using the two-stage step-up method of Benjamini *et al.* (34), where the FDR(Q) was set at 1%. This generates an FDR-adjusted p value (also termed q) in which significance (discovery) is $p < 0.01$.

Multiple-reaction monitoring liquid chromatography mass spectrometry of mitochondrial proteins

A tier 2 level, targeted proteomic analysis was described previously (35) and was used to quantify mitochondrial proteins between ACE 10/10⁻ and WT⁻ derived monocytes. Experimenters were not blinded to groups during processing or analysis. Monocyte pellets ($n = 4$ per mouse genotype, ACE 10/10 *versus* WT) were lysed in 8 M urea dissolved in 50 mM Tris-HCl buffer, pH 8.0. Lysis was facilitated by high-pressure treatment on a Pressure Biosciences (Easton, MA) barocycler (model 2320EXT), with 60 1-min cycles consisting of 50 s of 45,000 p.s.i. followed by 10 s at atmospheric pressure (ATM). Following extraction, protein concentration was assayed using Pierce BCA (Thermo Fisher Scientific). Fifty micrograms of protein from each sample were aliquoted for digestion, and each sample was reduced using 10 mM DTT (10 mM) and subsequently alkylated with iodoacetamide (100 mM). Samples were diluted with 200 mM ammonium bicarbonate buffer and supplemented with 10% acetonitrile, to a final urea concentration of <2 M. Trypsin was added at a ratio of 1 μ g to 50 μ g of total protein and subjected to an additional series of 60 cycles (45,000 p.s.i. for 50 s, ATM for 10 s) at 37 °C, after which samples were left to incubate at ATM overnight at 37 °C. Digestion was quenched with 1% TFA, and samples were desalted on Nest C18 tips (Nest Group, Southborough, MA). Peptides were dried to completion and resuspended in a solution of 0.1% formic acid in double-distilled H₂O into which a 1:250 dilution of stable isotope-labeled reference peptides derived for targeted mitochondrial protein analysis as described in detail (35) were added. A total of 8 μ g of digested peptides, injected twice as duplicate technical replicates, were separated on a Prominence UFLCXR HPLC system (Shimadzu Corp., Kyoto, Japan) with a Waters Xbridge BEH30 C18 2.1 mm \times 100 mm, 3.5- μ m column flowing at 0.25 ml/min and 36 °C coupled to a QTRAP[®] 6500 (SCIEX, Framingham, MA). Mobile phase A consisted of 2% acetonitrile, 98% water, and 0.1% formic acid, and mobile phase B consisted of 95% acetonitrile, 5% water, and 0.1% formic acid. After loading, the column was equilibrated with 5% B for 5 min. Peptides were then eluted over 30 min with a linear 5–35% gradient of buffer B. The column was washed with 98% B for 10 min and then returned to 5% B for 5 min before loading the next sample. A scheduled, targeted acquisition method optimized for each peptide was used to monitor fragments within a 2-min window of the optimized retention time. Raw data were processed using the Skyline software package (Skyline Daily, version 19.1.1.309) to select peak boundaries and quantify the area under the curve for each fragment monitored. Peptides were manually inspected in Skyline for quality and excluded from further analysis if no discernable peak was observed. Skyline automated peak integration was used to define peak boundaries. The full Skyline data file has been shared on the Panorama web server, including the data from acquired but excluded peptide peak

groups (<https://panoramaweb.org/6fp9tn.url>).⁴ After processing in Skyline, fragment level data were exported as comma-separated values and further processed using a custom R script (Table S3). Only fragments with $<40\%$ coefficient of variation (CV) across the heavy standard peptides were used for quantification. A table of the peptide sequences and individual fragments included in quantitative analysis is provided in Table S3, with %CV across all heavy observations, as well as across the endogenous technical replicates provided as separate tables. The abundance ratios of endogenous to heavy standard for all quantified fragments for each peptide from each protein were averaged, and peptide level abundance ratios were further averaged to yield a final abundance ratio for each of the proteins monitored. Precision of the protein level quantification across technical replicates is provided in the supporting data and had an average of 10.8 ± 8 protein level %CV across the data set. The technical replicate abundance ratio was averaged for each mouse to yield the final protein level measurements. Adjusted p values were also calculated using GraphPad Prism and two-way analysis of variance (ANOVA) with a Bonferroni multiple-comparison test.

Western blot analysis

Cells were washed three times with cold PBS and lysed with radioimmune precipitation assay buffer containing protease inhibitors. The polyvinylidene difluoride membranes were incubated with OXPHOS Rodent WB Antibody Mixture (Abcam (Cambridge, UK), catalogue no. ab110413), Tom20 rabbit mAb (Cell signaling, catalogue no. 42406), OPA1 rabbit mAb (Cell Signaling, catalogue no. 80471), MFF XP rabbit mAb (Cell Signaling, catalogue no. 84580), VDAC rabbit mAb (Cell Signaling, catalogue no. 4661), ATP5 β (Invitrogen, catalogue no. MA1-930), Glut1 rabbit mAb (Cell Signaling, catalogue no. 12939), Glut4 mouse mAb (Cell Signaling, catalogue no. 2213), and β -actin mouse mAb (Sigma, catalogue no. A3854). Protein bands were measured using an Odyssey IR imaging system ODYSSEY CLx (LI-COR Biosciences, Lincoln, NE). The fluorescence intensity was evaluated using Image Studio Lite version 5.2.

Measurement of mitochondrial number, size, and morphology

MitoTracker—Cells were cultured for 2 h and then centrifuged to obtain a supernatant-free cell pellet. This was resuspended in prewarmed staining solution (HBSS + 0.1% BSA) containing 200 nM MitoTracker[™] Green FM (Thermo Fisher Scientific). After incubation for 30 min at 37 °C and 5% CO₂, cells were rinsed three times with prewarmed PBS and studied using a CyAn[™] ADP flow analyzer (Beckman Coulter). Data were analyzed with FlowJo version 7.6.5.

Confocal analysis—For confocal imaging, cells were stained with 100 nM MitoTracker[™] Red CMXRos (Thermo Fisher Scientific) for 30–45 min in a CO₂ incubator. Cells were carefully washed with prewarmed PBS and then with PBS containing 2 or 4% formaldehyde for 30 min. After rinsing with PBS three times, the cells were permeabilized with 0.1% Triton X-100 at

⁴ Please note that the JBC is not responsible for the long-term archiving and maintenance of this site or any other third party hosted site.

ACE increases myeloid cellular ATP expression

room temperature for 20 min and washed three times with PBS. They were then incubated with Phalloidin-Green (Thermo Fisher Scientific) for 30 min, rinsed three times with PBS, and incubated with ProLong Gold Antifade Reagent with DAPI (Life Technologies) for 2–3 h. Fluorescence localization was observed using a Leica Sp5-X confocal microscope (Leica). Image analysis for the fluorescence localization was performed using LAS AF Lite (Leica). Data were processed by CellProfiler 3.0 and analyzed by GraphPad Prism software.

EM

Samples used for EM were processed using standard techniques. Briefly, samples were fixed with 2.5% EM grade glutaraldehyde in 0.1 M sodium cacodylate buffer (pH 7.4) at 37 °C. After fixation, samples were placed in 2% osmium tetroxide in 0.1 M sodium cacodylate buffer (pH 7.4), dehydrated, and embedded in Durcupan resin (Sigma-Aldrich). Ultimately, the samples were viewed using a JEOL 1010 transmission electron microscope at 80 kV and an AMT (Advanced Microscopy Techniques) XR80 digital camera. Image capture engine software was AMT version 7.00. The micrographs were taken at $\times 48,000$ magnification.

Mitochondrial membrane potential

Peritoneal macrophages were obtained 4 days after thioglycollate injection and were seeded on a plate overnight in medium C. The next morning, cells were removed by scraping and incubated with 100 nM TMRE (Abcam, catalogue no. ab113852) for 20 min at 37 °C. After one wash with PBS, mitochondrial membrane potential ($\Delta\psi_m$) was measured by flow cytometry using an excitation wavelength of 549 nm and measuring emissions at 575 nm.

Glucose uptake

Cells were treated with or without 500 μM 2-NBDG (Life Technologies, Inc.) in culture medium for 1 h at 37 °C with 5% CO_2 . For analysis by flow cytometry, cells were washed twice with ice-cold PBS and kept on ice. Cells were analyzed by flow cytometry within 30 min of harvest. The Glucose Uptake-Glo™ assay kit (Promega) was also used to measure cell glucose uptake as a second means of analysis. According to the manufacturer's instructions, cells were washed twice in PBS and then seeded into a 96-well plate (100,000/well). 2-Deoxyglucose was added and incubated for 10 min in glucose-free medium. During this period, 2-deoxyglucose is converted to 2-deoxyglucose 6-phosphate. This was measured in a coupled reaction producing luciferin.

Superoxide production by cytochrome *c* reduction

Superoxide production was measured by superoxide dismutase-inhibitable cytochrome *c* reduction (15). 1×10^6 cells were resuspended with 1 ml of medium H (145 mM NaCl, 5 mM KCl, 1 mM MgCl_2 , 0.8 mM CaCl_2 , 10 mM HEPES, 5 mM glucose, pH 7.4) containing 100 μM cytochrome *c* (Sigma). As a negative control, 15 μg of superoxide dismutase (Sigma) was added. 200 μl of the cell suspension was put in wells of a 96-well plate and stimulated with 5 μM PMA for superoxide production. Absorbance at 550 nm was recorded for 20 min with 1

measurement/min at 37 °C with gentle shaking. After subtracting the background values, superoxide production was calculated by using the absorption coefficient of $21 \text{ mM}^{-1} \text{ cm}^{-1}$ for cytochrome *c*. For experiments using oligomycin, the concentration of drug was 10 $\mu\text{g}/\text{ml}$.

Phagocytosis

Phagocytosis was measured in thioglycollate-elicited peritoneal macrophages using the Vybrant Phagocytosis Assay kit (Thermo Fisher Scientific) according to the manufacturer's protocol. Macrophages were cultured in medium C containing 10% FBS (for 500 ml: RPMI1640, 437 ml; stock penicillin/streptomycin (Gemini Bio-Products), 5 ml; sodium pyruvate (stock solution 100 mM), 2.5 ml; HEPES (stock solution 1 M), 5 ml; fetal bovine serum, 50 ml; 2-mercaptoethanol, 1.75 μl) for 2 h with fragments of fluorescein-labeled *E. coli* (K-12 strain) with or without oligomycin (10 $\mu\text{g}/\text{ml}$). Cells were then washed three times for 5 min each with FACS buffer (PBS with 2% FBS, 0.1% sodium azide, 1 mM EDTA) and stained with anti-mouse PE-CD11B antibody (Biolegend, catalogue no. 101207) and anti-mouse F4/80 BV421 antibody (Biolegend, catalogue no. 123131) at 4 °C for 1 h. After washing three times with FACS buffer, cells were stained with anti-rabbit APC (SouthernBiotech, catalogue no. 4050-11L). *E. coli* particles were measured by flow cytometry performed with a Sony SA38000 instrument, and data were analyzed with FlowJo version 10.4 (FlowJo, LLC, Ashland, OR). Analysis consisted of determining the green fluorescence from internalized *E. coli* in $\text{CD11b}^+ \text{F4/80}^+$ cells.

Respirometry and lactate efflux (Seahorse assay)

All experiments were conducted with a Seahorse XF96 or XFe96 analyzer. Peritoneal macrophages were cultured overnight on bacterial Petri dishes with medium C containing 1 ng/ml murine M-CSF (Peprotech). The next day, the macrophages were dislodged and spun onto Seahorse XF96 plates (600 \times g for 5 min) coated with Cell-Tak (Corning, catalogue no. C354240) according to the manufacturer's instructions at 1.5×10^5 cells/well. Measurements were conducted in DMEM (Sigma, catalogue no. D5030) supplemented with 5 mM HEPES, 8 mM glucose, 2 mM glutamine, and 2 mM pyruvate. Oligomycin (2 μM), FCCP (two sequential pulses of 500 nM), and rotenone (200 nM) with antimycin A (1 μM) were added acutely to the wells, and respiratory parameters were calculated as described (19). Lactate efflux was measured by correcting rates of extracellular acidification for (i) the scaling factor of the microplate sensor coverage and (ii) confounding respiratory acidification, and ATP production rates were calculated (36, 37). Permeabilization of the plasma membrane with perfringolysin O (Agilent Technologies, catalogue no. 102504-100) and analysis of cells in response to pyruvate/malate, glutamate/malate, and succinate/rotenone were performed in MAS buffer (70 mM sucrose, 220 mM mannitol, 10 mM KH_2PO_4 , 5 mM MgCl_2 , 2 mM HEPES, and 1 mM EGTA, pH 7.2) at 37 °C exactly as described previously (20, 21).

Macrophage lactic acid production

Thioglycollate-elicited peritoneal macrophages were collected and cultured with three different conditions: (i) medium

C containing 10% FBS and 4 g of glucose/liter), (ii) medium C without FBS, and (iii) medium C without FBS or glucose for 12 h. The collected medium was deproteinated using a kit from BioVison (K808-200) and the manufacturer's instructions. Lactate in 50 μ l of medium was then quantified using the AmplitudeTM fluorimetric L-lactate assay kit (AAT Bioquest, catalogue no. 13814), following the manufacturer's instructions. Fluorescence intensity was measured at 540-nm excitation/590-nm emission by a fluorescence plate reader.

Statistical analysis

All of the reported results were obtained from at least three independent experiments. One-way ANOVA and *t* test statistics were obtained using GraphPad Prism software. Statistical treatment of MS data is detailed in that section.

Author contributions—D.-Y. C., J. F. G., A. S. D., J. E. V. E., and K. E. B. conceptualization; D.-Y. C., W. R. S., A. E. J., E. A. B., D. O.-D., S. J. P., J. F. G., and A. S. D. resources; D.-Y. C., W. R. S., L. C. V., Z. K., A. E. J., S. S., S. J. P., J. F. G., A. S. D., and K. E. B. data curation; D.-Y. C., W. R. S., A. E. J., E. A. B., S. S., D. O.-D., S. J. P., J. F. G., and A. S. D. software; D.-Y. C., L. C. V., Z. K., Z. P., A. E. J., S. S., and A. S. D. formal analysis; D.-Y. C., A. E. J., D. O.-D., S. J. P., and A. S. D. validation; D.-Y. C., W. R. S., L. C. V., Z. K., Z. P., A. E. J., E. A. B., S. J. P., and A. S. D. investigation; D.-Y. C., A. E. J., S. J. P., and A. S. D. visualization; D.-Y. C., Z. P., A. E. J., E. A. B., and A. S. D. methodology; D.-Y. C., W. R. S., L. C. V., A. E. J., E. A. B., S. J. P., J. F. G., A. S. D., and K. E. B. writing-original draft; D.-Y. C., A. E. J., J. F. G., A. S. D., J. E. V. E., and K. E. B. writing-review and editing; A. E. J., D. O.-D., J. F. G., A. S. D., and K. E. B. supervision; A. E. J., S. J. P., A. S. D., J. E. V. E., and K. E. B. funding acquisition; A. S. D. project administration.

Acknowledgments—We thank Brian Taylor, Justin Z. Y. Shen, Dr. Roberta A. Gottlieb, Dr. Kolja Wawrowsky, Dr. Allen M. Andres, Dr. Mercury Y. Lin, and Dr. Mark Haas for advice and assistance in completing this study.

References

- Bernstein, K. E., Ong, F. S., Blackwell, W. L., Shah, K. H., Giani, J. F., Gonzalez-Villalobos, R. A., Shen, X. Z., Fuchs, S., and Touyz, R. M. (2013) A modern understanding of the traditional and nontraditional biological functions of angiotensin-converting enzyme. *Pharmacol. Rev.* **65**, 1–46 [CrossRef Medline](#)
- Mentz, R. J., Bakris, G. L., Waeber, B., McMurray, J. J., Gheorghiane, M., Ruilope, L. M., Maggioni, A. P., Swedberg, K., Piña, I. L., Fiuzat, M., O'Connor, C. M., Zannad, F., and Pitt, B. (2013) The past, present and future of renin-angiotensin aldosterone system inhibition. *Int. J. Cardiol.* **167**, 1677–1687 [CrossRef Medline](#)
- Bernstein, K. E., Khan, Z., Giani, J. F., Cao, D. Y., Bernstein, E. A., and Shen, X. Z. (2018) Angiotensin-converting enzyme in innate and adaptive immunity. *Nat. Rev. Nephrol.* **14**, 325–336 [CrossRef Medline](#)
- Lieberman, J. (1975) Elevation of serum angiotensin-converting-enzyme (ACE) level in sarcoidosis. *Am. J. Med.* **59**, 365–372 [CrossRef Medline](#)
- Baudin, B. (2002) New aspects on angiotensin-converting enzyme: from gene to disease. *Clin. Chem. Lab. Med.* **40**, 256–265 [CrossRef Medline](#)
- Brice, E. A., Friedlander, W., Bateman, E. D., and Kirsch, R. E. (1995) Serum angiotensin-converting enzyme activity, concentration, and specific activity in granulomatous interstitial lung disease, tuberculosis, and COPD. *Chest* **107**, 706–710 [CrossRef Medline](#)
- Lieberman, J., and Rea, T. H. (1977) Serum angiotensin-converting enzyme in leprosy and coccidioidomycosis. *Ann. Intern. Med.* **87**, 423–425 [CrossRef Medline](#)
- Olle, E. W., Deogracias, M. P., Messamore, J. E., McClintock, S. D., Barron, A. G., Anderson, T. D., and Johnson, K. J. (2007) Screening of serum samples from Wegener's granulomatosis patients using antibody microarrays. *Proteomics Clin. Appl.* **1**, 1212–1220 [CrossRef Medline](#)
- Weinstock, J. V. (1991) Production of neuropeptides by inflammatory cells within the granulomas of murine schistosomiasis mansoni. *Eur. J. Clin. Invest.* **21**, 145–153 [CrossRef Medline](#)
- Cronan, M. R., Beerman, R. W., Rosenberg, A. F., Saelens, J. W., Johnson, M. G., Oehlers, S. H., Sisk, D. M., Jurcic Smith, K. L., Medvitz, N. A., Miller, S. E., Trinh, L. A., Fraser, S. E., Madden, J. F., Turner, J., Stout, J. E., et al. (2016) Macrophage epithelial reprogramming underlies mycobacterial granuloma formation and promotes infection. *Immunity* **45**, 861–876 [CrossRef Medline](#)
- Danilov, S. M., Tikhomirova, V. E., Metzger, R., Naperova, I. A., Bukina, T. M., Goker-Alpan, O., Tayebi, N., Gayfullin, N. M., Schwartz, D. E., Samokhodskaya, L. M., Kost, O. A., and Sidransky, E. (2018) ACE phenotyping in Gaucher disease. *Mol. Genet. Metab.* **123**, 501–510 [CrossRef Medline](#)
- Diet, F., Pratt, R. E., Berry, G. J., Momose, N., Gibbons, G. H., and Dzau, V. J. (1996) Increased accumulation of tissue ACE in human atherosclerotic coronary artery disease. *Circulation* **94**, 2756–2767 [CrossRef Medline](#)
- Ohishi, M., Ueda, M., Rakugi, H., Naruko, T., Kojima, A., Okamura, A., Higaki, J., and Ogihara, T. (1997) Enhanced expression of angiotensin-converting enzyme is associated with progression of coronary atherosclerosis in humans. *J. Hypertens.* **15**, 1295–1302 [CrossRef Medline](#)
- Saijonmaa, O., Nyman, T., and Fyhrquist F. (2007) Atorvastatin inhibits angiotensin-converting enzyme induction in differentiating human macrophages. *Am. J. Physiol. Heart Circ. Physiol.* **292**, H1917–H1921 [CrossRef Medline](#)
- Khan, Z., Shen, X. Z., Bernstein, E. A., Giani, J. F., Eriguchi, M., Zhao, T. V., Gonzalez-Villalobos, R. A., Fuchs, S., Liu, G. Y., and Bernstein, K. E. (2017) Angiotensin-converting enzyme enhances the oxidative response and bactericidal activity of neutrophils. *Blood* **130**, 328–339 [CrossRef Medline](#)
- Shen, X. Z., Billet, S., Lin, C., Okwan-Duodu, D., Chen, X., Lukacher, A. E., and Bernstein, K. E. (2011) The carboxypeptidase ACE shapes the MHC class I peptide repertoire. *Nat. Immunol.* **12**, 1078–1085 [CrossRef Medline](#)
- Shen, X. Z., Li, P., Weiss, D., Fuchs, S., Xiao, H. D., Adams, J. A., Williams, I. R., Capecchi, M. R., Taylor, W. R., and Bernstein, K. E. (2007) Mice with enhanced macrophage angiotensin-converting enzyme are resistant to melanoma. *Am. J. Pathol.* **170**, 2122–2134 [CrossRef Medline](#)
- Okwan-Duodu, D., Datta, V., Shen, X. Z., Goodridge, H. S., Bernstein, E. A., Fuchs, S., Liu, G. Y., and Bernstein, K. E. (2010) Angiotensin-converting enzyme overexpression in mouse myelomonocytic cells augments resistance to *Listeria* and methicillin-resistant *Staphylococcus aureus*. *J. Biol. Chem.* **285**, 39051–39060 [CrossRef Medline](#)
- Divakaruni, A. S., Paradyse, A., Ferrick, D. A., Murphy, A. N., and Jastroch, M. (2014) Analysis and interpretation of microplate-based oxygen consumption and pH data. *Methods Enzymol.* **547**, 309–354 [CrossRef Medline](#)
- Divakaruni, A. S., Wiley, S. E., Rogers, G. W., Andreyev, A. Y., Petrosyan, S., Loviscach, M., Wall, E. A., Yadava, N., Heuck, A. P., Ferrick, D. A., Henry, R. R., McDonald, W. G., Colca, J. R., Simon, M. I., Ciaraldi, T. P., and Murphy, A. N. (2013) Thiazolidinediones are acute, specific inhibitors of the mitochondrial pyruvate carrier. *Proc. Natl. Acad. Sci. U.S.A.* **110**, 5422–5427 [CrossRef Medline](#)
- Divakaruni, A. S., Rogers, G. W., and Murphy, A. N. (2014) Measuring mitochondrial function in permeabilized cells using the Seahorse XF analyzer or a Clark-type oxygen electrode. *Curr. Protoc. Toxicol.* **60**, 25.2.1–16 [CrossRef Medline](#)
- Davies, L. C., Rice, C. M., McVicar, D. W., and Weiss, J. M. (2019) Diversity and environmental adaptation of phagocytic cell metabolism. *J. Leukoc. Biol.* **105**, 37–48 [CrossRef Medline](#)
- Antononkov, V. D., Isomursu, A., Mennerich, D., Vapola, M. H., Weiher, H., Kietzmann, T., and Hiltunen, J. K. (2015) The human mitochondrial DNA depletion syndrome gene MPV17 encodes a non-selective channel

ACE increases myeloid cellular ATP expression

- that modulates membrane potential. *J. Biol. Chem.* **290**, 13840–13861 [CrossRef Medline](#)
24. Khan, Z., Cao, D. Y., Giani, J. F., Bernstein, E. A., Veiras, L. C., Fuchs, S., Wang, Y., Peng, Z., Kalkum, M., Liu, G. Y., and Bernstein, K. E. (2019) Overexpression of the C-domain of angiotensin-converting enzyme reduces melanoma growth by stimulating M1 macrophage polarization. *J. Biol. Chem.* **294**, 4368–4380 [CrossRef Medline](#)
 25. Skeggs, L. T., Jr. (1993) Discovery of the two angiotensin peptides and the angiotensin converting enzyme. *Hypertension* **21**, 259–260 [CrossRef Medline](#)
 26. Bernstein, K. E., Koronyo, Y., Salumbides, B. C., Sheyn, J., Pelissier, L., Lopes, D. H., Shah, K. H., Bernstein, E. A., Fuchs, D. T., Yu, J. J., Pham, M., Black, K. L., Shen, X. Z., Fuchs, S., and Koronyo-Hamaoui, M. (2014) Angiotensin-converting enzyme overexpression in myelomonocytes prevents Alzheimer's-like cognitive decline. *J. Clin. Invest.* **124**, 1000–1012 [CrossRef Medline](#)
 27. Semis, M., Gugiu, G. B., Bernstein, E. A., Bernstein, K. E., and Kalkum, M. (2019) The plethora of angiotensin-converting enzyme-processed peptides in mouse plasma. *Anal. Chem.* **91**, 6440–6453 [CrossRef Medline](#)
 28. Lin, C., Datta, V., Okwan-Duodu, D., Chen, X., Fuchs, S., Alsabeh, R., Billet, S., Bernstein, K. E., and Shen, X. Z. (2011) Angiotensin-converting enzyme is required for normal myelopoiesis. *FASEB J.* **25**, 1145–1155 [CrossRef Medline](#)
 29. Jha, A. K., Huang, S. C., Sergushichev, A., Lampropoulou, V., Ivanova, Y., Loginicheva, E., Chmielewski, K., Stewart, K. M., Ashall, J., Everts, B., Pearce, E. J., Driggers, E. M., and Artyomov, M. N. (2015) Network integration of parallel metabolic and transcriptional data reveals metabolic modules that regulate macrophage polarization. *Immunity* **42**, 419–430 [CrossRef Medline](#)
 30. Mills, E. L., Kelly, B., Logan, A., Costa, A. S. H., Varma, M., Bryant, C. E., Tourlomousis, P., Däbritz, J. H. M., Gottlieb, E., Latorre, I., Corr, S. C., McManus, G., Ryan, D., Jacobs, H. T., Szibor, M., *et al.* (2016) Succinate dehydrogenase supports metabolic repurposing of mitochondria to drive inflammatory macrophages. *Cell* **167**, 457–470.e13 [CrossRef Medline](#)
 31. Pearce, E. L., and Pearce, E. J. (2013) Metabolic pathways in immune cell activation and quiescence. *Immunity* **38**, 633–643 [CrossRef Medline](#)
 32. Tannahill, G. M., Curtis, A. M., Adamik, J., Palsson-McDermott, E. M., McGettrick, A. F., Goel, G., Frezza, C., Bernard, N. J., Kelly, B., Foley, N. H., Zheng, L., Gardet, A., Tong, Z., Jany, S. S., Corr, S. C., *et al.* (2013) Succinate is an inflammatory signal that induces IL-1 β through HIF-1 α . *Nature* **496**, 238–242 [CrossRef Medline](#)
 33. Van den Bossche, J., O'Neill, L. A., and Menon, D. (2017) Macrophage immunometabolism: where are we (going)? *Trends Immunol.* **38**, 395–406 [CrossRef Medline](#)
 34. Benjamini, Y., Krieger, A. M., and Yekutieli, D. (2006) Adaptive linear step-up procedures that control the false discovery rate. *Biometrika* **93**, 491–507 [CrossRef](#)
 35. Stotland, A. B., Spivia, W., Orosco, A., Andres, A. M., Gottlieb, R. A., Van Eyk, J. E., and Parker, S. J. (2019) MitoPlex: a targeted multiple reaction monitoring assay for quantification of a curated set of mitochondrial proteins. *bioRxiv* [CrossRef](#)
 36. Romero, N., Swain, P., Neilson, A., and Dranka, B. P. (2017) Improving quantification of cellular glycolytic rate using Agilent Seahorse XF technology. Agilent Technologies White Paper
 37. Divakaruni, A. S., Wallace, M., Buren, C., Martyniuk, K., Andreyev, A. Y., Li, E., Fields, J. A., Cordes, T., Reynolds, I. J., Bloodgood, B. L., Raymond, L. A., Metallo, C. M., and Murphy, A. N. (2017) Inhibition of the mitochondrial pyruvate carrier protects from excitotoxic neuronal death. *J. Cell Biol.* **216**, 1091–1105 [CrossRef Medline](#)